Molecular Immunology 108 (2019) 34–44

Contents lists available at ScienceDirect

Molecular Immunology

journal homepage: www.elsevier.com/locate/molimm

Measuring anti-HLA antibody active concentration and affinity by surface plasmon resonance: Comparison with the luminex single antigen flow beads and T-cell flow cytometry crossmatch results

Jonathan Visentin[a,b,c,*], Damien Le Leu[b,c], Arend Mulder[d], Frédéric Jambon[b,c], Laure Badier[b,c], Jar-How Lee[e], Gwendaline Guidicelli[a], Charlène Bouthemy[a], Mamy Ralazamahaleo[a], Frans Claas[d], Carmelo Di Primo[f,g], Jean-Luc Taupin[a,b,c]

[a] CHU de Bordeaux, Laboratoire d'Immunologie et Immunogénétique, Hôpital Pellegrin, Place Amélie Raba Léon, Bordeaux, France
[b] Immuno ConcEpT, UMR CNRS 5164, 146 rue Léo Saignat, Bordeaux, France
[c] Université de Bordeaux, 146 rue Léo Saignat, Bordeaux, France
[d] Leiden University Medical Center, Department of Immunohaematology and Blood transfusion, Albinusdreef 2, 2300RC Leiden, the Netherlands
[e] One Lambda, Inc., 21001 Kittridge, Canoga Park, CA, USA
[f] Université de Bordeaux, Laboratoire ARNA, 146 rue Léo Saignat, Bordeaux, France
[g] INSERM U1212, CNRS UMR 5320, IECB, 2 rue Robert Escarpit, Pessac, France

ARTICLE INFO

Keywords:
Anti-HLA antibody
Surface plasmon resonance
Single antigen flow beads
Flow cytometry crossmatch
Active concentration
Affinity

ABSTRACT

Background: Although the Luminex single antigen flow beads (SAFB) and the flow cytometry crossmatch (FCXM) are the most sensitive assays used for anti-HLA antibodies characterization in transplant recipients, their semi-quantitative fluorescence read-out is not closely linked to graft outcome.
Methods: Surface plasmon resonance (SPR) was implemented to determine truly quantitative parameters of five human monoclonal anti-class I HLA antibodies (mAbs): first the active concentration and then the binding constants. The results were compared to those obtained with SAFB and T-cell FCXM (T-FCXM).
Results: The five mAbs displayed different rate and equilibrium constants for their cognate antigens. No correlation was evidenced between SAFB MFI or T-FCXM ratio and the binding parameters measured by SPR. Some mAbs amino acid substitutions within the epitope that influenced SAFB MFI resulted in affinity variations evidenced by SPR.
Conclusion: The SAFB MFI and T-FCXM ratio, both semi-quantitative parameters, only partially reflected the subtlety of the anti-HLA antibody/antigen interaction as it can be analyzed by SPR. Future clinical studies using SPR for anti-HLA antibodies characterization could bring novel insights into the understanding of HLA/anti-HLA interaction and therefore anti-HLA antibodies pathogenicity.

1. Introduction

The release of the Luminex Single Antigen Flow Beads (SAFB) assays was a major step forward in the management of organ recipients. These multiplex assays are very sensitive for IgG donor-specific anti-HLA antibodies (DSA) detection in recipients' serum (Wiebe et al., 2012; Guidicelli et al., 2016; Morrell et al., 2014; Visentin et al., 2016a; Smith et al., 2011). In the pre-transplantation setting, SAFB results can be confirmed using flow cytometry crossmatching (FCXM) (Visentin et al., 2016b). Both assays are often used in a semi-quantitative fashion, considering that the measured Mean Fluorescence Intensity (MFI) reflects the clinical "strength" of a DSA. However, many studies show that DSA MFI is not perfectly associated with graft outcomes (Wu et al., 2013; Lefaucheur et al., 2010; Courant et al., 2018; Salvadé et al.,

Abbreviations: a.a., amino acid; B2m, beta-2 microglobulin; CCFCA, capture calibration free concentration analysis; CFCA, calibration free concentration analysis; DSA, donor specific antibody(ies); FCXM, flow cytometry crossmatch; HLA, human leucocyte antigens; k_a, association rate constant; k_d, dissociation rate constant; K_D, dissociation equilibrium constant; mAb(s), monoclonal antibody(ies); MFI, mean fluorescence intensity; QC, quality control; RU, response units; SAFB, single antigen flow beads; SCK, single cycle kinetics; SPR, surface plasmon resonance

* Corresponding author at: CHU de Bordeaux, Laboratoire d'Immunologie et Immunogénétique, Hôpital Pellegrin, Place Amélie Raba Léon, 33076 Bordeaux Cedex, France.
E-mail address: jonathan.visentin@chu-bordeaux.fr (J. Visentin).

https://doi.org/10.1016/j.molimm.2019.02.006
Received 20 November 2018; Received in revised form 31 January 2019; Accepted 12 February 2019
Available online 16 February 2019

2016). Possible explanations are that SAFB and FCXM assays are difficult to standardize (Reed et al. (2013); Wu et al., 2013) and that SAFB assays suffer well-described positive (Morales-Buenrostro et al., 2008; Visentin et al., 2014a, 2015) and negative interferences (Schnaidt et al., 2011; Visentin et al., 2014b, c; Guidicelli et al., 2018) that introduce bias in clinical interpretations. Moreover, these assays do not routinely assess other antibody characteristics which are linked to Fc region, *e.g.* IgG subclass, which determine the effector response that will be induced (Freitas et al., 2013; Lefaucheur et al., 2016).

Besides these issues, other potential parameters possibly linking DSA MFI and pathogenicity have not been explored so far. Among them are the DSA active concentration and the affinity to their cognate HLA ligands, as well as antigen density and epitope availability on SAFB surface or on donor cells used for crossmatching. We recently developed a capture system to measure the active concentration and the affinity of anti-class I and DQ HLA antibodies by surface plasmon resonance (SPR) (Visentin et al., 2016d, 2018).

SPR-based biosensors can monitor in real time the binding of the antibody to its HLA target captured by a specific anchor immobilized onto the sensor chip (Jönsson et al., 1991; Fägerstam et al., 1992). Importantly, knowing the active concentration of the anti-HLA antibody, *i.e.* the fraction able to interact with the target, is a prerequisite for an accurate determination of the binding kinetics of the interaction and therefore of the dissociation equilibrium constant, which is equal to the ratio of the binding rates. However, calibration curves cannot be used for measuring anti-HLA antibody concentrations because antibodies are by nature almost all unique to a recipient (Duquesnoy, 2011). The Calibration Free Concentration Analysis (CFCA) approach has been developed for such situations (Christensen, 1997; Richalet-Sécordel et al., 1997). We successfully adapted it in a capture mode for measuring the active concentration of anti-HLA antibodies (Visentin et al., 2016d, 2018).

The binding of anti-HLA antibodies to their cognate antigens strongly depends on surface accessible polymorphic amino acids (a.a.) named by Duquesnoy et al." eplets" (Duquesnoy, 2011). Eplets are expected to engage most of the interaction strength between the antigen and the antibody. However, the contact surface between the antibody's paratope and the HLA molecule is larger than the sole eplet. The consequence is that other surface a.a., close enough to the eplet (15 Å), participate to the global epitope and to the interaction with the antibody's paratope. Then, when these a.a. vary between HLA alleles products sharing a same eplet, the binding kinetics of an antibody recognizing this eplet could be modified (Duquesnoy et al., 2013).

In this study, we measured by SPR the active concentration and the binding kinetics of five human monoclonal anti-HLA antibodies derived from allo-sensitized subjects. We then compared these results to those obtained from the routine SAFB and T-lymphocytes FCXM (T-FXCM) assays, taking into account epitope structural differences between HLA antigens.

2. Materials and methods

2.1. Antibodies and HLA molecules

The W6/32 and anti-B2m (clone B2M-01) mouse mAbs were purchased from ThermoFisher Scientific (Rockford, IL). The human mAbs were generated as previously described (Mulder et al., 2010). Their reactivities were previously determined by lymphocytotoxicity (Mulder et al., 2010) and/or SAFB assays (Duquesnoy et al., 2013; Mulder et al., 2010; Marrari et al., 2010). The SN230G6 (sentizing source HLA-A2 and HLA-B57), SN607D8 (sensitizing source HLA-A2), BRO11 F6 (sensitizing source unknown), DK7C11 (sensitizing source HLA-B45) and ROU9A6 (sensitizing source HLA-B44) clones recognize the 62GE, 142 T/145H, 144TKR + 151H, 167ES and 41 T eplets, respectively. They were produced in the form of hybridoma supernatants, purified on protein G resin (ThermoFisher Scientific), concentrated and buffer-exchanged in phosphate buffered saline with 0.05% Tween (PBS-T) with Amicon Ultra-4 10 kDa centrifugal filter units (Merck Millipore, Darmstadt, Germany). The purified HLA molecules (One Lambda Inc., Canoga Park, CA) were dialyzed against PBS-T with a 20 kDa cut-off Float-A-Lyzer G2 device (Spectrum Laboratories, Rancho Dominguez, CA).

2.2. Surface plasmon resonance experiments

SPR experiments were performed at 25 °C with a Biacore™ T200 apparatus (GE Healthcare Life Sciences, Uppsala, Sweden) on CM5 sensorchips (Biacore™), as described previously (Visentin et al., 2016d). An anti-beta2-microglobulin (anti-B2m) mouse mAb (clone B2M-01, ThermoFisher Scientific, Rockford, IL), was immobilized by amine coupling using a mixture of N-hydroxysuccinimide and N-ethyl-N'-dimethylaminopropyl carbodiimide according to the manufacturer's instructions (GE Healthcare), after dilution in a 10 mM sodium acetate buffer, pH 5, followed by an injection of 1 M ethanolamine, pH 8.5 (GE Healthcare) to deactivate the sensor chip surface. The sensorgrams were analyzed with the Biacore T200 Evaluation Software. A flow cell left blank was used for double-referencing of the sensorgrams (Myszka, 1999), *i.e.* the sensorgrams from the flow cell left blank and the sensorgram obtained with the blank were subtracted from the sensorgram obtained with the mAbs. Spikes still present at the beginning and at the end of the injection after this step were not removed because they did not affect the results, as previously shown (Di Primo, 2008; Palau and Di Primo, 2012). HLA antigens to be captured and mAbs were prepared in PBS-T (Sigma-Aldrich), which constituted the running buffer. Capture CFCA (CCFCA) and Single Cycle Kinetics (SCK) experiments were performed as described previously (Visentin et al., 2016d). All the samples and blanks were injected in duplicate.

Briefly, one cycle of CFCA experiment consisted in 1) capturing a high amount of the HLA targets to favour mass transport limitation conditions [> 1000 response units (RU)], 2) injecting the mAbs or blank (*i.e.* PBS-T) for 50 s at 5 or 100 µl/min and then 3) regenerating the surface with a 1 min pulse of 10 mM glycine pH 2.1 (GE Healthcare). After regeneration, the anti-B2m was still active allowing new CFCA cycles to be performed. Concentration measurements validation criteria recommended by Biacore are a sufficiently high initial binding rate at low flow (for example, higher than 0.3 RU/s at 5 µl/min) and slopes of the association phase of the sensorgrams sufficiently different, as reflected by a quality control (QC) ratio higher than 0.2. However we previously showed that lower QC ratio (> 0.15) are still acceptable and give reliable active concentration values (Visentin et al., 2016d).

One cycle of SCK experiment consisted in, 1) capturing a low amount of the HLA targets (< 100 RU) to avoid kinetic artifacts, 2) injecting the mAbs or blank (*i.e.* PBS-T) at 25 µl/min at 3 successive increasing concentrations with no regeneration between each injection, 3) one dissociation phase with running buffer only flowed for at least 5 min at 25 µl/min in order to monitor the mAb dissociation reaction and then 4) regenerating the surface with a 1 min pulse of 10 mM glycine pH 2.1 (GE Healthcare). After regeneration, the anti-B2m was still active which allowed new SCK cycles to be performed. The association and dissociation rate constants, k_a and k_d, respectively, were determined by direct curve fitting of the sensorgrams to a Langmuir 1:1 model of interaction, as described previously (Palau and Di Primo, 2012). The dissociation equilibrium constant, K_D, was calculated as k_d/k_a.

2.3. Total protein and IgG concentration assays

The total protein concentration of purified and concentrated mAbs was determined using an acid bicinchoninic assay (BCA) (Pierce TM BCA Protein Assay Kit, Thermo Scientific, Rockford, USA). The total IgG concentration was determined using the Human IgG ELISA

Quantitation Set from Bethyl Laboratories (Montgomery, USA). The providers' recommendations were strictly followed and average values from experiments performed in duplicate were used.

2.4. Luminex single antigen beads experiments

The LABScreen® Single Antigen Class I kits were from One Lambda. Mabs were used in human serum in order to mimic the assay's usual matrix. This serum was from a healthy male volunteer who had never been transfused nor transplanted. Before the addition of mAbs, the serum was EDTA-treated in order to avoid the complement interference/prozone phenomenon,as previously described (Schnaidt et al., 2011; Visentin et al., 2014b). The PE-labeled Goat Anti-Human IgG antibody (One Lambda) was used at a 1:100 dilution, as recommended by the manufacturer. MFI values for mAbs were normalized values by subtraction of MFI obtained with the serum alone.

2.5. T-lymphocyte FCXM assays

The T-FCXM assays were performed on freshly drawn total lymph node, spleen or blood mononuclear cells. MAb/cell pairs were selected to react against one HLA-A or -B donor antigen only. The mAbs were diluted in the same serum as for SAFB, without EDTA-treatment. The negative control was this serum alone. T-FCXM were performed according to our routine procedure (Visentin et al., 2016b; Couzi et al., 2011). The results were expressed as the ratio MFI between MFI obtained with the mAbs diluted in serum and MFI obtained with the normal serum used to dilute the mAb.

2.6. Sequence alignment and structural analysis tools

Amino acid sequence alignments were performed with the IMGT sequence alignment tool (http://www.ebi.ac.uk/ipd/imgt/hla/align.html). Residue localization and antibody accessibility were evaluated with the "space fill" command of the Cn3D structure software program (Hogue, 1997) using HLA-A*02:01 (MMDB ID: 82223, PDB ID: 3MGT) or HLA-B*52:01 (MMDB ID: 107517, PDB ID: 3W39) as a model downloaded from Entrez Molecular Modeling Database on the National Center for Biotechnology Information website (http://www.ncbi.nlm.nih.gov/Structure).

3. Results

3.1. SPR active concentration measurement and kinetic analysis of anti-HLA mAbs

The active concentrations of the five mAbs, *i.e.* the biologically active fraction of the mAbs present in solution that recognizes the immobilized target, were determined by CCFCA (Table 1). Fig. 1 shows that the sensorgrams were consistent with the mass transport limitation required for measuring active concentrations by SPR. Indeed, the initial binding rates at low flow rate (5 µl/min) were sufficiently different from those obtained at high flow rate (100 µl/min), as reflected by a QC ratio higher than 0.15 for all 5 mAbs (Table 1). The values obtained by this method were compared with the total protein and IgG concentrations determined by BCA and ELISA IgG assays, respectively (ratio BCA/CCFCA and ELISA/CCFCA in Table 1). With BCA, the total protein concentrations were 3.2 to 4.7-fold higher than the active concentrations, while IgG concentration with ELISA were 1.3 to 2-fold higher. We then determined the association and dissociation rate constants, k_a and k_d, respectively, and the dissociation equilibrium constant, K_D, for these mAbs/HLA complexes. The sensorgrams presented in Fig. 2 show that the fit to the 1:1 model of interaction was good and reproducible for SN230G6, SN607D8, ROU9A6 and DK7C11. We observed a slightly lower quality for BRO11 F6. The measured k_a, k_d and K_D are listed in Table 2. DK7C11 displayed the highest affinity followed by SN230G6, SN607D8, BRO11 F6 and ROU9A6. The impact of concentrations difference between CCFCA and BCA or ELISA assays on K_D measurements are also shown in SDC, Table 1 for an individual SCK experiment.

3.2. Comparison of SAFB and SPR results for the alleles assayed by SPR

Each of the five mAbs was analyzed with SAFB at five different concentrations corresponding to 10 K_D, 3 K_D, K_D, 1/3 K_D and 1/10 K_D values. For all mAbs, MFI increased with concentration (Fig. 3A), with the highest MFI being obtained for the 10 K_D concentration, but reaching different levels depending on the mAbs. The anti-B44 ROU9A6 displayed the highest MFI, followed by the anti-A2 SN203G6 and SN607D8 of very close MFI, slightly higher than for the anti-A11 BRO11 F6, and with far behind the anti-B44 DK7C11. An alternative plot of these data showed that at a given mAb concentration, MFI did not strictly mirror mAb affinity (Fig. 3B). Indeed, DK7C11 provided the lowest MFI values despite displaying the highest affinity for its target. In contrast, ROU9A6 displayed higher MFI than BRO11 F6 and identical MFI to SN607D8, despite its lower affinity. For SN230G6 and SN607D8, MFI was consistent with their affinity difference. Overall, we did not observe any significant correlation between SAFB MFI and the binding parameters measured by SPR (SDC, Fig. 1A–C).

3.3. SAFB and SPR results variations are linked to epitope structural differences

We then compared for each mAb the SAFB MFI obtained for each of the alleles they bound to, *i.e.* those with MFI > 500 at the 10 K_D concentration (Fig. 4). The mean MFI obtained with W6/32 and anti-beta2-microglobulin (B2m) mAbs at 1 µg/ml was used to approximate native HLA antigen density on each bead in order to refine the interpretation of MFI. We also investigated a.a. within 15 Å distance from

Table 1
Active concentration of the five mAbs measured by capture CFCA. The difference between active concentrations measured with CCFCA and total protein or IgG measurements performed with acid bicinchoninic and ELISA IgG assays, respectively, are shown as a ratio.

mAb	HLA target	Assay	Dilution	Measured active concentration (nM)	QC ratio[a]	Sample concentration (nM) ± SD	Concentration ratio : total protein / active	Concentration ratio : total IgG / active
SN230G6	A*02:01	1	1000	2.1	0.503	2150 ± 70	3.26	1.32
		2		2.2	0.471			
SN607D8	A*02:01	1	1000	6.1	0.176	5900 ± 354	4.67	1.42
		2	2000	2.8	0.176			
BRO11 F6	A*11:01	1	1000	2.4	0.232	2450 ± 70	3.16	1.31
		2		2.5	0.203			
ROU9A6	B*44:02	1	1000	1.2	0.191	1200 ± 0	4.54	1.98
		2		1.2	0.181			
DK7C11	B*44:02	1	1000	1.7	0.255	1700 ± 0	3.78	1.46
		2		1.7	0.242			

[a] The QC ratio reflects the degree of mass transport limitation.

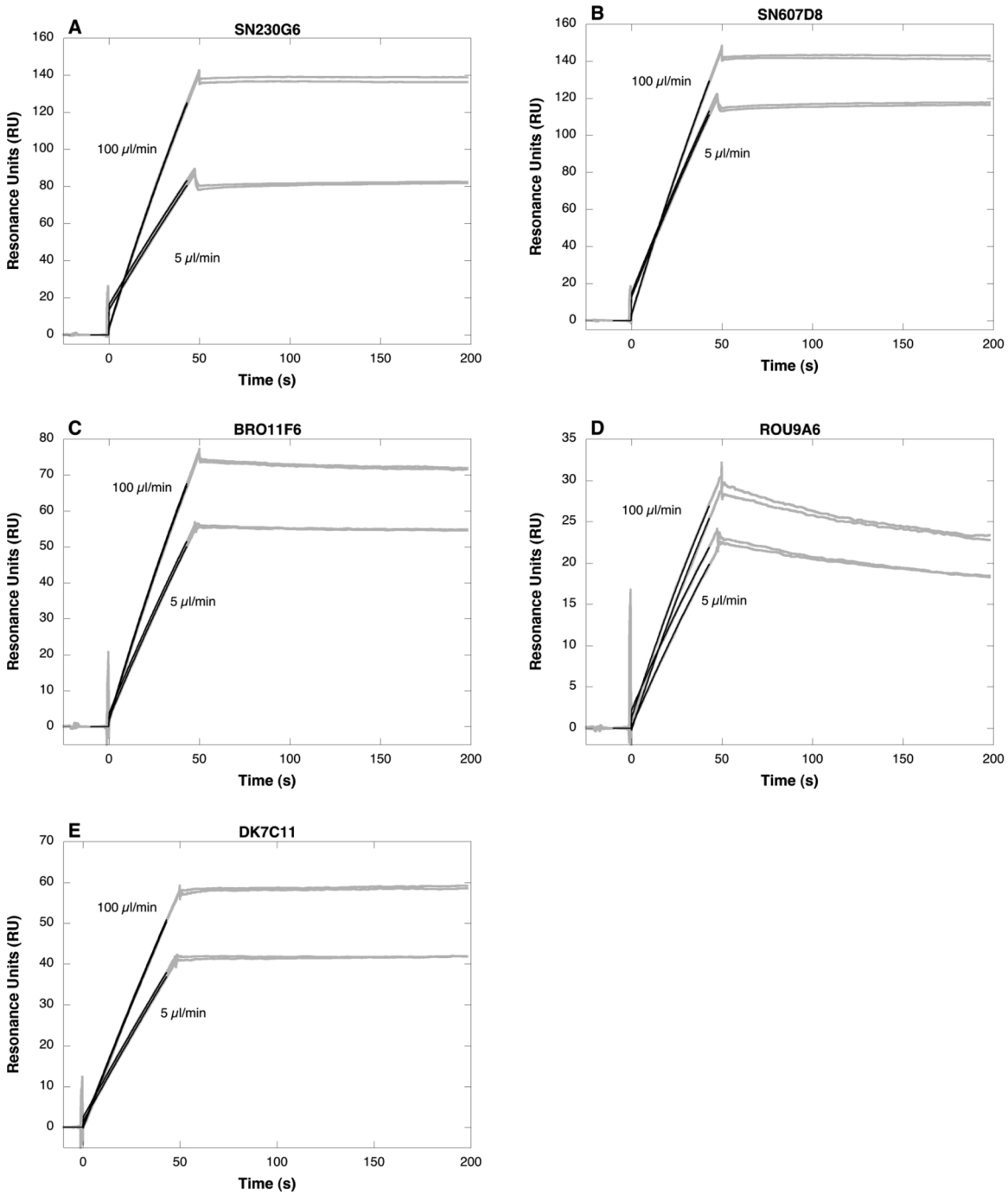

Fig. 1. CCFCA sensorgrams of mAbs active concentration measurement. A high amount (12 000 RU) of anti-B2m mAb was immobilized on a CM5 sensor chip. More than 1 000 RU of HLA targets were captured. The human mAbs were injected in duplicate for 50 s at 5 and 100 µl/min against HLA-A*02:01 (SN230G6, panel A, and SN607D8, panel B), HLA-A*11:01 (BRO11 F6, panel C) and HLA-B*44:02 (ROU9A6, panel D et DK7C11, panel E). Grey lines represent the experimental data and those in black the fit of the sensorgrams.

the targeted eplet in order to identify the differences between alleles that could impact on antibody recognition.

The SN230G6 mAb recognized six alleles' products (Fig. 4 and SDC, Table 2). We identified two 66 K/N and 163 T/I substitutions within this epitope that apparently had no impact on antibody recognition in SAFB assay, as MFI was comparable for all six alleles (SDC, Table 2 and Fig. 5). The binding kinetics of SN230G6 for A*02:03 were almost identical to those for A*02:01, while the affinity was 3-fold higher for B*57:01 (Table 3 and SDC, Fig. 2).

The SN607D8 mAb recognized six alleles' products (Fig. 4 and SDC, Table 3). The two 149 A/T and 152 V/E substitutions were present only in A*02:03 and probably modified antibody recognition in SAFB, as the MFI was significantly lower for this allele (SDC, Table 3 and Fig. 5). The binding kinetics of SN607D8 for A*68:01 were almost identical to those for A*02:01, while the affinity was 2.5-fold lower for A*02:03 (Table 3 and SDC, Fig. 3).

The BRO11 F6 mAb recognized seven alleles' products, which could be subdivided into three groups regarding their SAFB MFI (Fig. 4 and SDC, Table 4). We identified substitutions at positions 127, 150 and 152 that could modify antibody recognition (SDC, Table 4 and Fig. 5). The binding kinetics of BRO11 F6 for A*03:01 (intermediate MFI group) and A*01:01 (low MFI group) evidenced affinities respectively 3-fold and

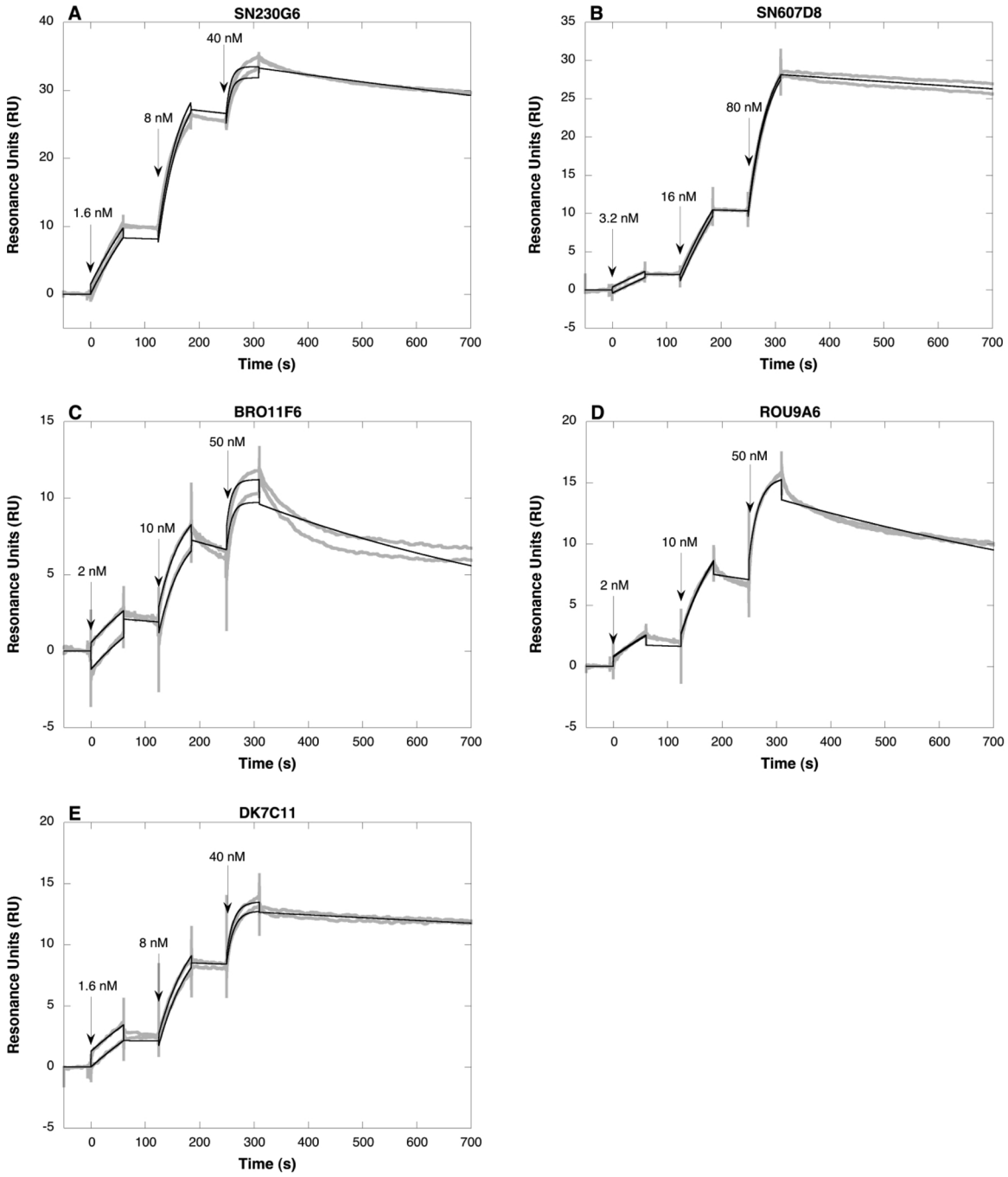

Fig. 2. Capture SCK sensorgrams of mAbs kinetic experiments. A high amount (12 000 RU) of anti-B2m mAb was immobilized on a CM5 sensor chip. Less than 100 RU of HLA-A*02:01 (SN230G6, SN607D8), A*11:01 (BRO11 F6) or B*44:02 (ROU9A6, DK7C11) were then captured in order to perform capture SCK. The samples were injected in duplicate at increasing concentrations for 60 s at 25 µl/min, without regeneration step between each injection. The association and dissociation rate constants, k_a and k_d, respectively, were determined by fitting the sensorgrams to a Langmuir 1:1 model of interaction. Grey lines represent the experimental data and those in black the fit of the sensorgrams.

Table 2
Rate and equilibrium constants for mAbs binding to captured HLAs. Three different class I HLA alleles were captured with an immobilized anti-beta2-microglobulin antibody. The association rate and the dissociation rate, k_a and k_d, respectively, were determined from direct curve fitting of the sensorgrams. The dissociation equilibrium constant, K_D, was calculated as k_d/k_a. The experiments were performed in duplicate, at least three times for all mAbs.

mAb	HLA target	k_a ($M^{-1}s^{-1}$) ± SD	k_d (s^{-1}) ± SD	K_D (M) ± SD
SN230G6	**A*02:01**	$3.5 \times 10^6 \pm 7.2 \times 10^5$	$3.7 \times 10^{-4} \pm 1.3 \times 10^{-4}$	$1.1 \times 10^{-10} \pm 5.3 \times 10^{-11}$
SN607D8	**A*02:01**	$7.0 \times 10^5 \pm 1.1 \times 10^5$	$1.6 \times 10^{-4} \pm 2.4 \times 10^{-5}$	$2.3 \times 10^{-10} \pm 6.7 \times 10^{-11}$
BRO11 F6	**A*11:01**	$7.7 \times 10^6 \pm 1.3 \times 10^7$	$3.2 \times 10^{-3} \pm 4.8 \times 10^{-3}$	$4.2 \times 10^{-10} \pm 1.2 \times 10^{-10}$
ROU9A6	**B*44:02**	$1.1 \times 10^6 \pm 2.3 \times 10^4$	$8.0 \times 10^{-4} \pm 8.3 \times 10^{-5}$	$7.1 \times 10^{-10} \pm 7.4 \times 10^{-11}$
DK7C11	**B*44:02**	$2.5 \times 10^6 \pm 4.5 \times 10^5$	$1.7 \times 10^{-4} \pm 3.3 \times 10^{-5}$	$7.0 \times 10^{-11} \pm 2.2 \times 10^{-11}$

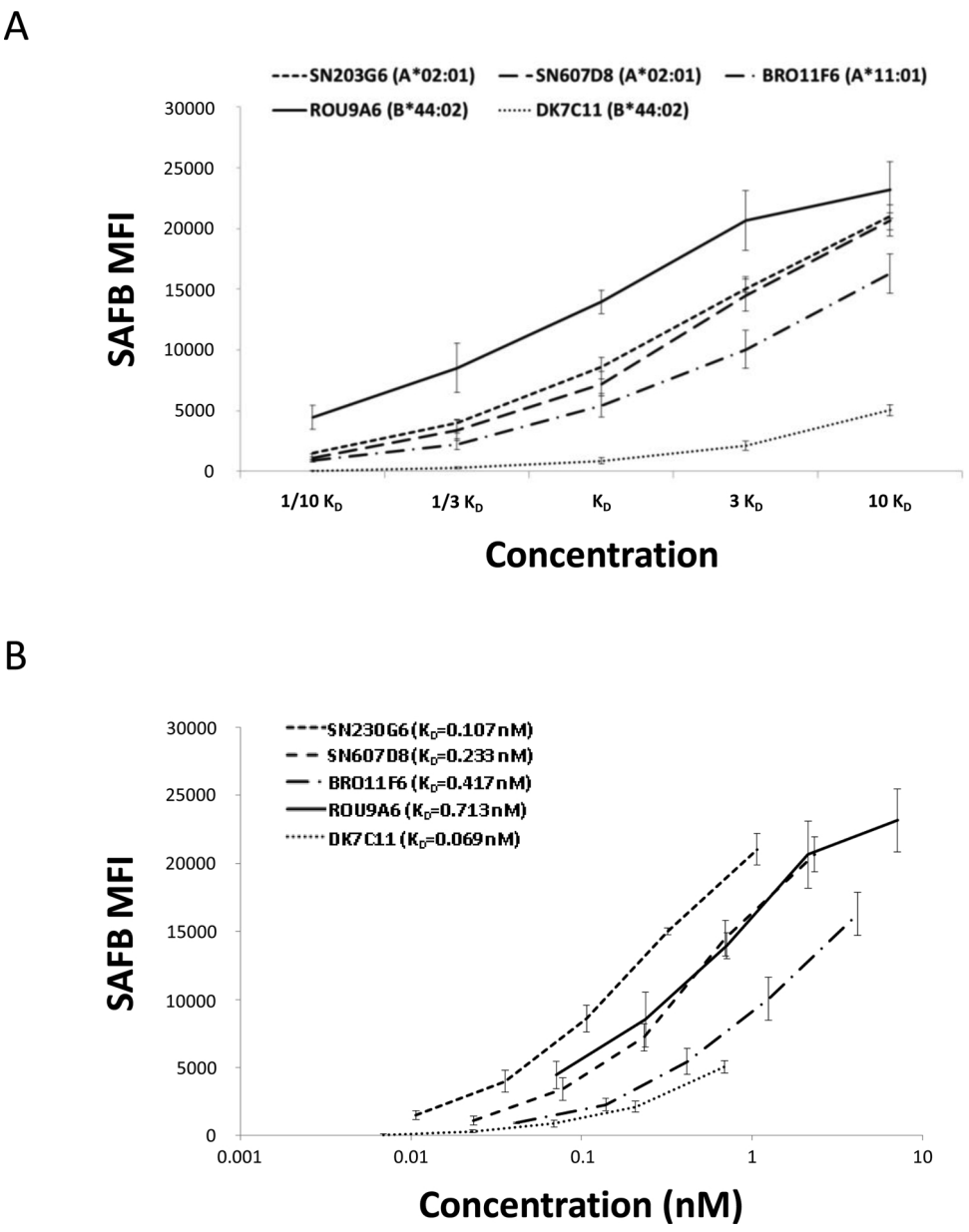

Fig. 3. Comparison with SAFB of the anti-HLA mAbs reactivity at the quantitative level. The five mAbs were tested with SAFB at five different concentrations corresponding to 10 K_D, 3 K_D, K_D, 1/3 K_D and 1/10 K_D, in human serum treated with EDTA (n = 3). Only the MFI obtained on the bead coated with the antigenic target used in SPR experiments are shown. A) SAFB MFI (mean +/- SD) related to the multiples of K_D used for each individual mAb. B) SAFB MFI (mean +/- SD) related to the concentrations used for each individual mAb.

10-fold lower than those for A*11:01 (high MFI group) (Table 3 and SDC, Fig. 4).

The ROU9A6 mAb recognized nineteen alleles' products, which could be subdivided into two groups according to their MFI range (Fig. 4 and SDC, Table 5). Alleles of the low MFI group differed for the eplet a.a. (41 T *versus* 41 A, respectively) (SDC, Table 5 and Fig. 5). Among the high MFI group alleles, only B*13:01 and B*13:02 had substitutions in the eplet vicinity (45 K/M and 46E/A) that did not impact antibody recognition further, as the SAFB MFI for these alleles was not different from that measured for the others. The binding kinetics of ROU9A6 were almost identical for B*44:02, B*45:01 and B*13:02, all three belonging to group 1, while we observed almost no SPR signal for B*15:12 and B*57:01 from group 2 (Table 3 and SDC, Fig. 5).

The DK7C11 mAb recognized five alleles' products (Fig. 4 and SDC, Table 6). Noteworthy, B*15:12 differed at the eplet positions 166D/E and 167 S/G, yet it provided an MFI comparable to that for B*44:02, B*44:03 and B*45:01 (SDC, Table 6 and Fig. 5). In contrast, allele B*82:01 had two substitutions in the eplet vicinity (69 T/A and 162 G/D) and provided lower SAFB MFI. The binding kinetics of DK7C11 were almost identical for B*44:02, B*45:01 and B*15:12, while the affinity was 4-fold lower for B*82:01 (Table 3 and SDC, Fig. 6).

3.4. Comparison with T-FCXM reactivity

Using lymphocytes from 50 different organ donors, 54 T-FCXM assays were performed to evaluate the mAbs reactivity against 16 different class I antigens. The mAbs were tested at concentrations similar to those used for SAFB assays. For the HLA targets first used in SPR experiments, we observed a concentration-dependent MFI signal-to-noise ratio increase but not all the mAbs provided comparable MFI increase as concentration raised. Indeed, ROU9A6 and BRO11 F6

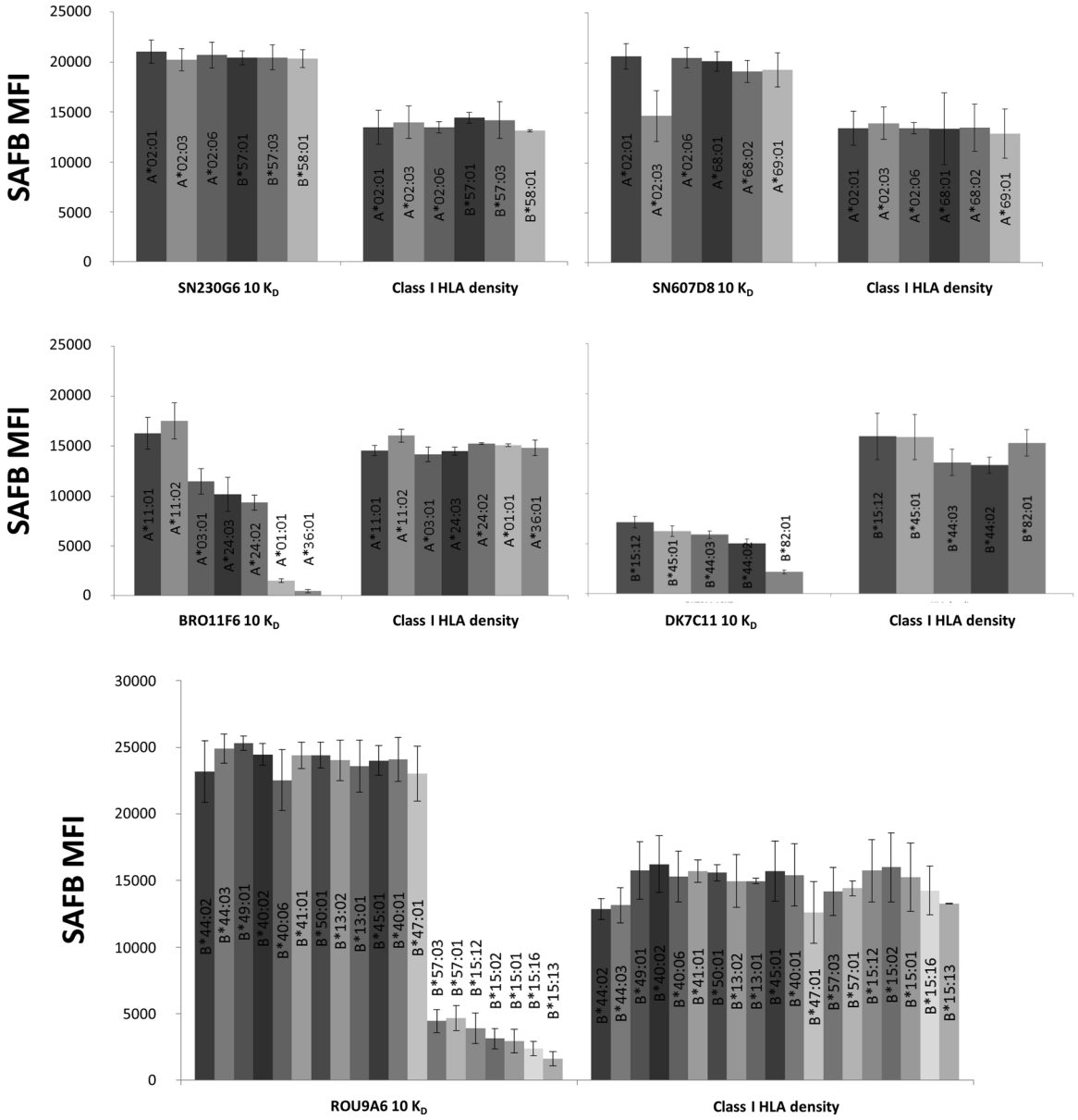

Fig. 4. Comparison of SAFB MFI provided by the recognized HLA alleles. The five mAbs were tested with SAFB at a concentration corresponding to 10 $K_{D,}$ in human serum treated with EDTA (n = 3). The SAFB MFI (mean +/- SD) obtained with all the alleles they recognized (MFI > 500) are shown. Comparison of HLA density at the surface of the different beads was normalized according to the MFI (mean +/- SD) obtained with W6/32 and anti-B2m mAbs at 1 µg/ml concentration.

displayed the highest MFI ratios towards B44 and A11 respectively, followed by SN607D8 towards A2, and with far behind SN230G6 and DK7C11 towards A2 and B44, respectively (Fig. 6A). In line with this, at a given mAb concentration, the MFI ratio did not strictly follow mAb affinity (Fig. 6B). Indeed, BRO11 F6, which displayed the second lowest affinity provided the highest T-FCXM MFI ratio at all concentrations, whereas the 4 other mAbs were not different between each other despite their distinct affinities. Overall, we did not observe any significant correlation between T-FCXM ratio and the binding parameters measured by SPR (SDC, Fig. 1D–F), neither with SAFB MFI (SDC, Fig. 1G). We also compared for BRO11 F6 and ROU9A6 the T-FCXM MFI ratios obtained according to the reactivity groups deduced from the SAFB assays and we observed consistent results (Fig. 6C and D, respectively). The results for each individual antigen/mAb combination are presented in SDC, Table 7.

4. Discussion

To our knowledge, the present study is the first one attempting to analyze the relationship between SAFB or T-FCXM assays and the active concentration and the binding parameters (rate and equilibrium constants) determined by SPR. Importantly, the active concentration determined by the SPR-based CFCA only relies on the change of initial binding rates with varying flow rates, under conditions of limited mass transport. Therefore, the SPR signal only results from the biologically active fraction of the mAb present in solution that recognizes the immobilized target. Knowing this concentration is mandatory to accurately determine the rate and equilibrium constants of the HLA/mAb complexes (Visentin et al., 2016d). In contrast, the widely used spectroscopic, colorimetric or nephelemetric methods give the total protein concentration in solution, *i.e.* also measure potentially unfolded and/or degraded forms as well as contaminants (Daga et al., 2017; Di Primo et al., 2017). Then, as anticipated, using total protein or IgG concentrations instead of the true active concentration has an impact on

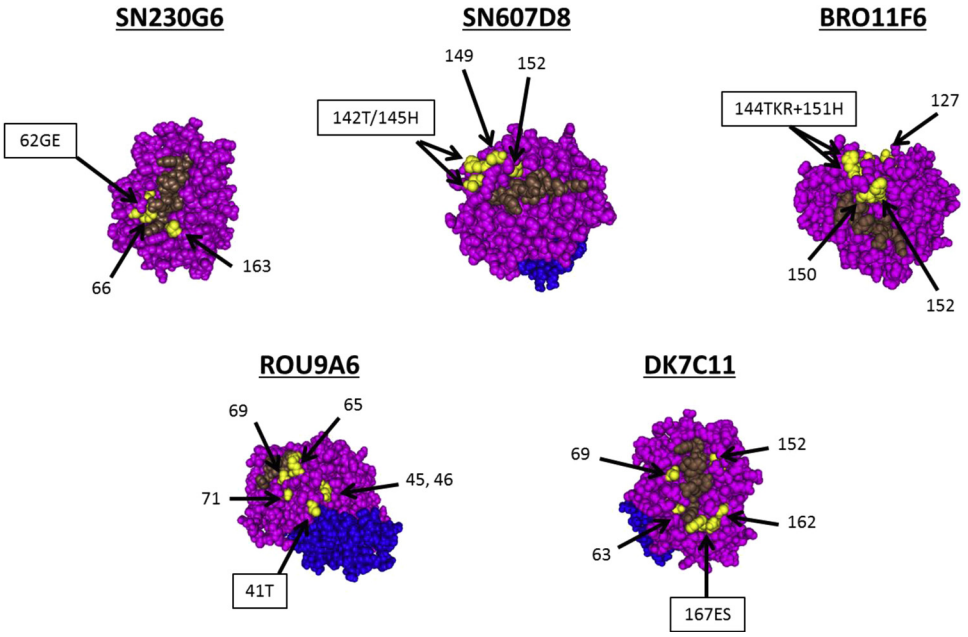

Fig. 5. Polymorphic and surface accessible amino-acid positions within a radius of 15 Å from the eplets recognized by the mAbs. Class I HLA molecules observed through different perspectives with the "space fill" command of the Cn3D structure software program, using HLA-A*02:01 or HLA-B*52:01 as a structural model, when appropriated. The HLA heavy chain, beta-2 microglobulin and peptide are colored in purple, blue and brown respectively. Amino acid positions of interest are highlighted in yellow, *i.e.* the eplets (boxed text) recognized by the mAbs and polymorphic and surface accessible a.a. positions located within a 15 Å distance from the eplet (For interpretation of the references to colour in this figure legend, the reader is referred to the web version of this article).

the determination of the K_D despite the use of any mAbs purification process (Daga et al., 2017; Di Primo et al., 2017; Daga et al., 2018).

We first observed that the five mAbs displayed different rate and equilibrium constants for their cognate antigens. This result was not surprising knowing the potentially infinite repertoire of anti-HLA antibodies raised by different individuals. Noteworthy, only one human mAb displayed a higher affinity for its cognate antigens than the prototypic anti-class I HLA clone W6/32 that we characterized in a previous work (Visentin et al., 2016d) and displays a K_D about 7.2×10^{-11} M. It is possible that the xenogenic origin of the W6/32 allowed for a more efficient affinity maturation of the humoral response, *e.g.* considering a higher immunogenicity of major histocompatibility antigens between species. Indeed, in an allogenic context, knowing the structural promiscuity existing between HLA proteins, the immune tolerance mechanisms that take place into the germinal centre could have negatively selected auto-reactive B cell clones (Linton et al., 1991; Notidis et al., 2002; Cyster et al., 1994) which could also produce antibodies with very high affinity for foreign HLA molecules. An alternative explanation could be that the alloreactive mAbs generation process that started with B cells immortalization by Epstein-Barr virus transformation, followed by cell fusion and cloning, did not always selected the clone displaying the highest affinity in each individual.

We then tested these mAbs with SAFB and T-FCXM assays using concentrations encompassing the K_D values, expecting similar SAFB MFI for all the mAbs at each individual point. The K_D being the concentration that saturates half of the binding sites on the target bead, a 10-fold higher concentration is expected to saturate more than 90% of the binding sites. Interestingly, the results were highly hetereogeneous between the mAbs as the SAFB MFI neither followed the range of their affinity nor the range of their association and dissociation rate constants. It has been proposed for multiplex assays such as the SAFB, but not proved yet, that increasing the number of alleles sharing a specific eplet can decrease SAFB MFI by diluting the serum antibody load on more targets (Tait et al., 2013). This could not explain our findings as ROU9A6 displayed the highest MFI despite its eplet being expressed by more SAFB than any other tested human mAb. Our hypothesis is that

Table 3
Rates and equilibrium constants of the mAbs for different HLA alleles. Several class I HLA alleles were captured with an immobilized anti-beta2-microglobulin antibody. The association rate and the dissociation rate, k_a and k_d, respectively, were determined from direct curve fitting of the sensorgrams. The dissociation equilibrium constant, K_D, was calculated as k_d/k_a. The experiments were performed in duplicate and two times for all mAbs. Results from HLA A*02:01, A*11:01 and B*44:02 were those already shown in Table 2. ND: not determined because no signal.

mAb	HLA target	k_a ($M^{-1}s^{-1}$) ± SD	k_d (s^{-1}) ± SD	K_D (M) ± SD
SN230G6	**A*02:01**	$3.5 \times 10^6 \pm 7.2 \times 10^5$	$3.7 \times 10^{-4} \pm 1.3 \times 10^{-4}$	$1.1 \times 10^{-10} \pm 5.3 \times 10^{-11}$
	A*02:03	$3.8 \times 10^6 \pm 5.4 \times 10^5$	$5.4 \times 10^{-4} \pm 5.4 \times 10^{-5}$	$1.4 \times 10^{-10} \pm 5.3 \times 10^{-12}$
	B*57:01	$5.9 \times 10^6 \pm 1.3 \times 10^6$	$2.0 \times 10^{-4} \pm 2.3 \times 10^{-5}$	$3.3 \times 10^{-11} \pm 2.3 \times 10^{-12}$
SN607D8	**A*02:01**	$7.0 \times 10^5 \pm 1.1 \times 10^5$	$1.6 \times 10^{-4} \pm 2.4 \times 10^{-5}$	$2.3 \times 10^{-10} \pm 6.7 \times 10^{-11}$
	A*02:03	$5.1 \times 10^6 \pm 9.4 \times 10^5$	$3.0 \times 10^{-3} \pm 5.3 \times 10^{-4}$	$5.7 \times 10^{-10} \pm 4.9 \times 10^{-12}$
	A*68:01	$1.3 \times 10^6 \pm 1.6 \times 10^5$	$4.0 \times 10^{-4} \pm 6.3 \times 10^{-5}$	$3.1 \times 10^{-10} \pm 8.6 \times 10^{-11}$
BRO11 F6	**A*11:01**	$7.7 \times 10^6 \pm 1.3 \times 10^7$	$3.2 \times 10^{-3} \pm 4.8 \times 10^{-3}$	$4.2 \times 10^{-10} \pm 1.2 \times 10^{-10}$
	A*03:01	$9.0 \times 10^5 \pm 3.5 \times 10^5$	$1.1 \times 10^{-3} \pm 2.0 \times 10^{-4}$	$1.3 \times 10^{-9} \pm 3.0 \times 10^{-10}$
	A*01:01	$5.6 \times 10^6 \pm 3.5 \times 10^5$	$2.3 \times 10^{-2} \pm 2.1 \times 10^{-5}$	$4.2 \times 10^{-9} \pm 2.6 \times 10^{-10}$
ROU9A6	**B*44:02**	$1.1 \times 10^6 \pm 2.3 \times 10^4$	$8.0 \times 10^{-4} \pm 8.3 \times 10^{-5}$	$7.1 \times 10^{-10} \pm 7.4 \times 10^{-11}$
	B*45:01	$8.3 \times 10^6 \pm 7.9 \times 10^6$	$5.0 \times 10^{-3} \pm 5.0 \times 10^{-3}$	$6.1 \times 10^{-10} \pm 4.2 \times 10^{-11}$
	B*13:02	$3.0 \times 10^6 \pm 1.4 \times 10^6$	$1.9 \times 10^{-3} \pm 6.3 \times 10^{-4}$	$6.2 \times 10^{-10} \pm 8.7 \times 10^{-11}$
	B*15:12	ND	ND	ND
	B*57:01	ND	ND	ND
DK7C11	**B*44:02**	$2.5 \times 10^6 \pm 4.5 \times 10^5$	$1.7 \times 10^{-4} \pm 3.3 \times 10^{-5}$	$7.0 \times 10^{-11} \pm 2.2 \times 10^{-11}$
	B*45:01	$2.4 \times 10^6 \pm 4.5 \times 10^4$	$1.9 \times 10^{-4} \pm 1.0 \times 10^{-5}$	$7.8 \times 10^{-11} \pm 5.8 \times 10^{-12}$
	B*15:12	$2.8 \times 10^6 \pm 1.4 \times 10^5$	$3.1 \times 10^{-4} \pm 3.0 \times 10^{-6}$	$1.1 \times 10^{-10} \pm 6.5 \times 10^{-12}$
	B*82:01	$3.5 \times 10^6 \pm 1.9 \times 10^5$	$9.9 \times 10^{-4} \pm 3.4 \times 10^{-5}$	$2.8 \times 10^{-10} \pm 2.5 \times 10^{-11}$

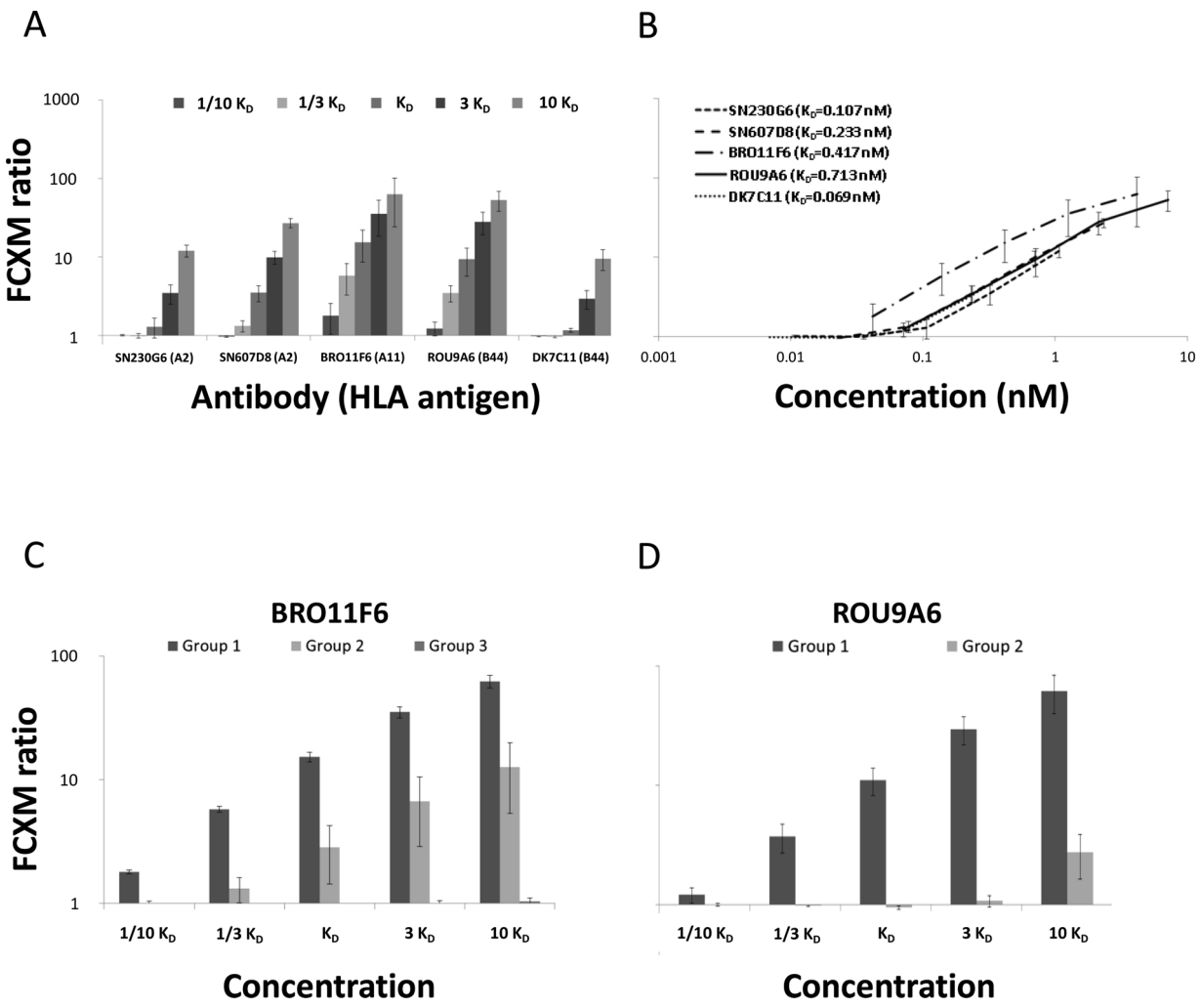

Fig. 6. Comparison with FCXM of the anti-HLA mAbs reactivity at the quantitative level. The five mAbs were tested in human serum with T-FCXM at five different concentrations corresponding to 10 K_D, 3 K_D, K_D, 1/3 K_D and 1/10 K_D. A) T-FCXM ratio (mean +/- SD) according to the multiples of K_D used for each individual mAb. B) T-FCXM ratio (mean +/- SD) according to the concentrations used for each individual mAb. For A and B, only the ratio obtained on the bead coated with the antigenic target used in SPR experiments are shown. C) T-FXCM ratio (mean +/- SD) obtained with the antigens from the different reactivity groups previously identified with SAFB for BRO11 F6. D) T-FXCM ratio (mean +/- SD) obtained with the antigens from the different reactivity groups previously identified with SAFB for ROU9A6.

the accessibility of HLA epitopes on SAFB might differ between alleles, depending on the spatial orientation of the antigen and/or the mode of binding to the bead surface. Some steric hindrance phenomena outside the paratope/epitope contact zone could also exist for peculiar alleles sharing the same eplet.

The design of the SAFB assay should most probably not be incriminated because we used for SPR the same recombinant proteins, although attached in a different manner onto the surface. In addition, comparable heterogeneity was also observed for the T-FCXM cellular assay relying on naturally produced cell bound HLA molecules, yet the mAbs reactivity range differed from the one obtained with SAFB. Noteworthy, interpreting the T-FCXM results might be more complex as HLA surface expression naturally seems to vary, depending on the HLA antigen and between donors (Hönger et al., 2015; René et al., 2015). For SAFB, the opposite is true. The amount of antigen immobilized is imposed by the manufacturer and is homogenous across a given production lot. In line with this, the standard deviations for T-FCXM stainings were higher than for SAFB assays. Nevertheless, we cannot exclude a role for a different topography of HLA distribution or spatial disposition between cell surface and SAFB. Here again some HLA epitopes could be more or less available depending on the experimental setting, explaining why a perfect correlation between SAFB MFI and T-FCXM ratios does not exist (Visentin et al., 2016b). Strikingly, with the exception of BRO11 F6 we observed that, despite displaying different affinities, the mAbs provided very similar FCXM ratio when used at the same concentration (Fig. 5B). It is conceivable that the impact of quite little differences in terms of binding constants is overtaken by other limiting or synergistic phenomenons, such as mAbs diffusion across the extracellular matrix down to the cell surface or binding reinforcement through avidity, respectively. Indeed, major differences between SPR and SAFB/T-FCXM endpoint assays are the constant replacement of the analyte at the contact of the antigen, the real-time assessment of interaction and the use of conditions avoiding avidity phenomenon for SPR.

For each mAb we compared the SAFB MFI obtained with all its bead targets and, depending on the mAbs, not all of them displayed the same MFI. The heterogeneity among the beads was more pronounced for BRO11 F6 and ROU9A6, allowing several reactivity groups to be determined. Interestingly, the same patterns were observed with T-FCXM and SPR. This is of crucial importance as it indicates that large differences in binding constants values had an impact on cell recognition strength.

The study of surface accessible polymorphic a.a. positions in the eplets vicinity identified several substitutions potentially able to alter

mAbs reactivity. However, some of them were neither associated with MFI nor with binding kinetics changes. Their physico-chemical properties, size and position might be of great importance (Duquesnoy et al., 2013; Kosmoliaptsis et al., 2011; Mallon et al., 2015). As an example, the DK7C11 bound with similar rate and equilibrium constants and also provided similar SAFB MFI with B*44:02 and B*15:12 alleles, probably because the 166D/E and 167S/G substitutions are physico-chemically conservative. It was the opposite for the B*82:01 allele which bears the two non-conservative 69 T/A and 162 G/D substitutions in the eplet vicinity. We observed similar behavior with the SN607D8 interacting with HLA-A*02:03 in comparison with A*02:01 or A*68:01, and also with the BRO11 F6 interacting with A*01:01, then A*03:01 and A*11:01.

The ROU9A6 was also highly informative, as it provided similar kinetics constants and SAFB MFI with B*44:02 and B*13:02, even if the latter has non physico-chemically conservative substitutions in the eplet vicinity (45 K/M and 46E/A). On the contrary, the group 2 alleles differing in the a.a. constituting the eplet itself (41 T/A) had a very low SAFB MFI in comparison with B*44:02. We studied two of them by SPR and could not measure any interaction. Interestingly, other antigens with 41 A were absolutely negative in SAFB. We did not find a clear explanation yet it can be anticipated that the polymorphic a.a. of these alleles situated in the vicinity of the eplet play a role.

The SN230G6 was a counter-example, displaying a higher affinity for B*57:01 than for A*02:01 or A*02:03 despite similar SAFB MFI for all these alleles. As the binding strength of this mAb for HLA-A2 alleles was very high, it is possible that increasing affinity above a certain level does not translate into any measurable difference in SAFB assay. Finally, it has been described that peptide presented by HLA alleles can play a role in antibody binding (Mulder et al., 2005). As HLA molecules used in this study were produced in cell lines expressing a classical immunopeptidome, it is unlikely that the numerous peptides presented by the different HLA alleles were a major reason for the different mAbs reactivities. Yet SPR could be an interesting tool to explore this field.

The aim of this study was to determine if there was a tight association between the anti-HLA mAbs binding parameters measured by SPR and the results obtained with assays classicaly used in histocompatibility laboratories. If yes, this would mean that further characterization of anti-HLA antibodies by SPR would most probably be useless in clinical practice. Of note, patient's humoral alloreactivity would lead to the production of polyclonal anti-HLA antibodies. Then, the relationship between active concentration, binding kinetics, SAFB MFI and FCXM ratio of anti-HLA antibodies from patients' sera would be even more complex. Nevertheless, we recently determined the active concentrations and binding kinetics of HLA antibodies from recipients sensitized against various HLA-DQ antigens (Visentin et al., 2018) and we obtained results similar to mAbs, *i.e.* no direct correlation between SAFB MFI and the active concentrations or the binding constants determined by SPR.

We believe that SPR-based assays will not replace the very useful SAFB and FCXM assays. Indeed, SPR does not allow a precise characterization of the multiple HLA antigens targeted by serum antibodies as quickly as SAFB does. SPR assays cannot be used either in emergency situations as SAFB and FCXM assays can. However, it could constitute a complementary assay performed in 1–2 working days, fully compatible with the clinical practice (Visentin et al., 2018), to refine the characterization of DSA identified by the routine assays.

5. Conclusion

The SAFB and FCXM assays barely reflect the subtlety of anti-HLA antibody recognition as it can be characterized by SPR, the gold-standard biophysical method for measuring active concentrations, binding rates and equilibrium constants. These findings likely explain the poor correlation that exists between these routinely assays used currently and recipients' clinical outcomes. Future steps will aim to determine in large cohorts if concentration and binding kinetics of donor specific anti-HLA antibodies could bring insights on our understanding of anti-HLA antibodies pathogenicity.

Author's contribution

J.T., J.V. and C.D.P. contributed to the design of the study. J.T., J.V. and C.D.P. participated in the writing of the paper. J.V., D.L., L.B., F.J., G.G., M.R., C.B., C.D.P. and J.T. participated in the performance of the research. J.T., J.V. and C.D.P. participated in data analysis. A.M., J.H.L. and F.C. were involved in critical revision of the manuscript.

Disclosure

The University of Bordeaux, the Bordeaux's University Hospital, the CNRS and the INSERM have filed a patent application on the use of SPR to study anti-HLA antibodies in allosensitized patients' sera. J. Visentin, JL. Taupin and C. Di Primo are listed as inventors on this patent. J-H Lee is an employee of One Lambda Inc. The other authors of this manuscript have no conflicts of interest to disclose.

Fundings

This work has benefited from a grant given by Astellas Pharma France. The funders had no role in work design and analysis, decision to publish, or preparation of the manuscript.

Acknowledgments

This work has benefited from the facilities and expertises of the Biophysical and Structural Chemistry plateform (BPCS) at the European Institute of Chemistry and Biology (IECB), CNRS UMS3033, Inserm US001, University of Bordeaux (http://www.iecb.ubordeaux.fr/index.php/fr/plateformestechnologiques). The Biacore T200 instrument used for the experiment was acquired with the support of the Conseil Régional d'Aquitaine, the GIS-IBiSA, and the Cellule Hôtels à Projets of the CNRS. The authors thank Lætitia Minder, assistant engineer at the IECB, and also the technicians of the immunology laboratory for their technical assistance and expertise.

Appendix A. Supplementary data

Supplementary material related to this article can be found, in the online version, at doi:https://doi.org/10.1016/j.molimm.2019.02.006.

References

Christensen, L.L., 1997. Theoretical analysis of protein concentration determination using biosensor technology under conditions of partial mass transport limitation. Anal. Biochem. 249 (2), 153–164. https://doi.org/10.1006/abio.1997.2182.

Courant, M., Visentin, J., Linares, G., et al., 2018. The disappointing contribution of anti-human leukocyte antigen donor-specific antibodies characteristics for predicting allograft loss. Nephrol. Dial. Transpl. Off. Publ. Eur. Dial. Transpl. Assoc. – Eur. Ren. Assoc. 33 (10), 1853–1863. https://doi.org/10.1093/ndt/gfy088.

Couzi, L., Araujo, C., Guidicelli, G., et al., 2011. Interpretation of positive flow cytometric crossmatch in the era of the single-antigen bead assay. Transplantation 91 (5), 527–535. https://doi.org/10.1097/TP.0b013e31820794bb.

Cyster, J.G., Hartley, S.B., Goodnow, C.C., 1994. Competition for follicular niches excludes self-reactive cells from the recirculating B-cell repertoire. Nature 371 (6496), 389–395. https://doi.org/10.1038/371389a0.

Daga, S., Moyse, H., Briggs, D., et al., 2017. Direct quantitative measurement of the kinetics of HLA-specific antibody interactions with isolated HLA proteins. Hum. Immunol.(October). https://doi.org/10.1016/j.humimm.2017.10.012.

Daga, S., Moyse, H., Briggs, D., et al., 2018. Response to the comments on "Direct quantitative measurement of the kinetics of HLA-specific antibody interactions with isolated HLA proteins.". Hum. Immunol. 79 (2), 130–131. https://doi.org/10.1016/j.humimm.2017.12.001.

Di Primo, C., 2008. Real time analysis of the RNAI-RNAII-Rop complex by surface plasmon resonance: from a decaying surface to a standard kinetic analysis. J. Mol. Recognit. JMR 21 (1), 37–45. https://doi.org/10.1002/jmr.860.

Di Primo, C., Taupin, J.-L., Visentin, J., 2017. Comments on "Direct quantitative

measurement of the kinetics of HLA-specific antibody interactions with isolated HLA proteins.". Hum. Immunol.(November). https://doi.org/10.1016/j.humimm.2017.11.009.
Duquesnoy, R.J., 2011. Humoral alloimmunity in transplantation: relevance of HLA epitope antigenicity and immunogenicity. Front. Immunol. 2, 59. https://doi.org/10.3389/fimmu.2011.00059.
Duquesnoy, R.J., Marrari, M., Jelenik, L., Zeevi, A., Claas, F.H.J., Mulder, A., 2013. Structural aspects of HLA class I epitopes reacting with human monoclonal antibodies in Ig-binding, C1q-binding and lymphocytotoxicity assays. Hum. Immunol. 74 (10), 1271–1279. https://doi.org/10.1016/j.humimm.2013.05.016.
Fägerstam, L.G., Frostell-Karlsson, A., Karlsson, R., Persson, B., Rönnberg, I., 1992. Biospecific interaction analysis using surface plasmon resonance detection applied to kinetic, binding site and concentration analysis. J. Chromatogr. 597 (1-2), 397–410.
Freitas, M.C.S., Rebellato, L.M., Ozawa, M., et al., 2013. The role of immunoglobulin-G subclasses and C1q in de novo HLA-DQ donor-specific antibody kidney transplantation outcomes. Transplantation 95 (9), 1113–1119. https://doi.org/10.1097/TP.0b013e3182888db6.
Guidicelli, G., Guerville, F., Lepreux, S., et al., 2016. Non-complement-Binding de novo donor-specific Anti-HLA antibodies and kidney allograft survival. J. Am. Soc. Nephrol. JASN 27 (2), 615–625. https://doi.org/10.1681/ASN.2014040326.
Guidicelli, G., Visentin, J., Franchini, N., et al., 2018. Prevalence, distribution and amplitude of the complement interference phenomenon in single antigen flow beads assays. HLA(March). https://doi.org/10.1111/tan.13263.
Hogue, C.W., 1997. Cn3D: a new generation of three-dimensional molecular structure viewer. Trends Biochem. Sci. 22 (8), 314–316.
Hönger, G., Krähenbühl, N., Dimeloe, S., Stern, M., Schaub, S., Hess, C., 2015. Inter-individual differences in HLA expression can impact the CDC crossmatch. Tissue Antigens 85 (4), 260–266. https://doi.org/10.1111/tan.12537.
Jönsson, U., Fägerstam, L., Ivarsson, B., et al., 1991. Real-time biospecific interaction analysis using surface plasmon resonance and a sensor chip technology. BioTechniques 11 (5), 620–627.
Kosmoliaptsis, V., Dafforn, T.R., Chaudhry, A.N., Halsall, D.J., Bradley, J.A., Taylor, C.J., 2011. High-resolution, three-dimensional modeling of human leukocyte antigen class I structure and surface electrostatic potential reveals the molecular basis for alloantibody binding epitopes. Hum. Immunol. 72 (11), 1049–1059. https://doi.org/10.1016/j.humimm.2011.07.303.
Lefaucheur, C., Loupy, A., Hill, G.S., et al., 2010. Preexisting donor-specific HLA antibodies predict outcome in kidney transplantation. J. Am. Soc. Nephrol. JASN 21 (8), 1398–1406. https://doi.org/10.1681/ASN.2009101065.
Lefaucheur, C., Viglietti, D., Bentlejewski, C., et al., 2016. IgG donor-specific anti-human HLA antibody subclasses and kidney allograft antibody-mediated injury. J. Am. Soc. Nephrol. JASN 27 (1), 293–304. https://doi.org/10.1681/ASN.2014111120.
Linton, P.J., Rudie, A., Klinman, N.R., 1991. Tolerance susceptibility of newly generating memory B cells. J. Immunol. Baltim. Md. 1950 146 (12), 4099–4104.
Mallon, D.H., Bradley, J.A., Winn, P.J., Taylor, C.J., Kosmoliaptsis, V., 2015. Three-dimensional structural modelling and calculation of electrostatic potentials of HLA Bw4 and Bw6 epitopes to explain the molecular basis for alloantibody binding: toward predicting HLA antigenicity and immunogenicity. Transplantation 99 (2), 385–390. https://doi.org/10.1097/TP.0000000000000546.
Marrari, M., Mostecki, J., Mulder, A., Claas, F., Balazs, I., Duquesnoy, R.J., 2010. Human monoclonal antibody reactivity with human leukocyte antigen class I epitopes defined by pairs of mismatched eplets and self-eplets. Transplantation 90 (12), 1468–1472. https://doi.org/10.1097/TP.0b013e3182007b74.
Morales-Buenrostro, L.E., Terasaki, P.I., Marino-Vázquez, L.A., Lee, J.-H., El-Awar, N., Alberú, J., 2008. Natural" human leukocyte antigen antibodies found in non-alloimmunized healthy males. Transplantation 86 (8), 1111–1115. https://doi.org/10.1097/TP.0b013e318186d87b.
Morrell, M.R., Pilewski, J.M., Gries, C.J., et al., 2014. De novo donor-specific HLA antibodies are associated with early and high-grade bronchiolitis obliterans syndrome and death after lung transplantation. J. Heart Lung Transpl. Off. Publ. Int. Soc. Heart Transpl. 33 (12), 1288–1294. https://doi.org/10.1016/j.healun.2014.07.018.
Mulder, A., Eijsink, C., Kester, M.G.D., et al., 2005. Impact of peptides on the recognition of HLA class I molecules by human HLA antibodies. J. Immunol. Baltim. Md. 1950 175 (9), 5950–5957.
Mulder, A., Kardol, M.J., Arn, J.S., et al., 2010. Human monoclonal HLA antibodies reveal interspecies crossreactive swine MHC class I epitopes relevant for xenotransplantation. Mol. Immunol. 47 (4), 809–815. https://doi.org/10.1016/j.molimm.2009.10.004.
Myszka, D.G., 1999. Improving biosensor analysis. J. Mol. Recognit. JMR 12 (5), 279–284. https://doi.org/10.1002/(SICI)1099-1352(199909/10)12:5<279::AID-JMR473>3.0.CO;2-3.
Notidis, E., Heltemes, L., Manser, T., 2002. Dominant, hierarchical induction of peripheral tolerance during foreign antigen-driven B cell development. Immunity 17 (3), 317–327.
Palau, W., Di Primo, C., 2012. Single-cycle kinetic analysis of ternary DNA complexes by surface plasmon resonance on a decaying surface. Biochimie 94 (9), 1891–1899. https://doi.org/10.1016/j.biochi.2012.04.025.
Reed, E.F., Rao, P., Zhang, Z., et al., 2013. Comprehensive assessment and standardization of solid phase multiplex-bead arrays for the detection of antibodies to HLA. Am. J. Transpl. Off. J. Am. Soc. Transpl. Am. Soc. Transpl. Surg. 13 (7), 1859–1870. https://doi.org/10.1111/ajt.12287.
René, C., Lozano, C., Villalba, M., Eliaou, J.-F., 2015. 5' and 3' untranslated regions contribute to the differential expression of specific HLA-A alleles. Eur. J. Immunol. 45 (12), 3454–3463. https://doi.org/10.1002/eji.201545927.
Richalet-Sécordel, P.M., Rauffer-Bruyère, N., Christensen, L.L., Ofenloch-Haehnle, B., Seidel, C., Van Regenmortel, M.H., 1997. Concentration measurement of unpurified proteins using biosensor technology under conditions of partial mass transport limitation. Anal. Biochem. 249 (2), 165–173. https://doi.org/10.1006/abio.1997.2183.
Salvadé, I., Aubert, V., Venetz, J.-P., et al., 2016. Clinically-relevant threshold of preformed donor-specific anti-HLA antibodies in kidney transplantation. Hum. Immunol. 77 (6), 483–489. https://doi.org/10.1016/j.humimm.2016.04.010.
Schnaidt, M., Weinstock, C., Jurisic, M., Schmid-Horch, B., Ender, A., Wernet, D., 2011. HLA antibody specification using single-antigen beads–a technical solution for the prozone effect. Transplantation 92 (5), 510–515. https://doi.org/10.1097/TP.0b013e31822872dd.
Smith, J.D., Banner, N.R., Hamour, I.M., et al., 2011. De novo donor HLA-specific antibodies after heart transplantation are an independent predictor of poor patient survival. Am. J. Transpl. Off. J. Am. Soc. Transplant. Am. Soc. Transpl. Surg. 11 (2), 312–319. https://doi.org/10.1111/j.1600-6143.2010.03383.x.
Tait, B.D., Süsal, C., Gebel, H.M., et al., 2013. Consensus guidelines on the testing and clinical management issues associated with HLA and non-HLA antibodies in transplantation. Transplantation 95 (1), 19–47. https://doi.org/10.1097/TP.0b013e31827a19cc.
Visentin, J., Guidicelli, G., Bachelet, T., et al., 2014a. Denatured class I human leukocyte antigen antibodies in sensitized kidney recipients: prevalence, relevance, and impact on organ allocation. Transplantation 98 (7), 738–744. https://doi.org/10.1097/TP.0000000000000229.
Visentin, J., Vigata, M., Daburon, S., et al., 2014b. Deciphering complement interference in anti-human leukocyte antigen antibody detection with flow beads assays. Transplantation 98 (6), 625–631. https://doi.org/10.1097/TP.0000000000000315.
Visentin, J., Guidicelli, G., Moreau, J.-F., Lee, J.-H., Taupin, J.-L., 2015. Deciphering allogeneic antibody response against native and denatured HLA epitopes in organ transplantation. Eur. J. Immunol. 45 (7), 2111–2121. https://doi.org/10.1002/eji.201445340.
Visentin, J., Chartier, A., Massara, L., et al., 2016a. Lung intragraft donor-specific antibodies as a risk factor for graft loss. J. Heart Lung Transpl. Off. Publ. Int. Soc. Heart Transpl. 35 (12), 1418–1426. https://doi.org/10.1016/j.healun.2016.06.010.
Visentin, J., Bachelet, T., Borg, C., et al., 2016b. Reassessment of t lymphocytes crossmatches results prediction with luminex class I single antigen flow beads assay. Transplantation(June). https://doi.org/10.1097/TP.0000000000001239.
Visentin, J., Guidicelli, G., Couzi, L., et al., 2016c. Deciphering IgM interference in IgG anti-HLA antibody detection with flow beads assays. Hum. Immunol. 77 (11), 1048–1054. https://doi.org/10.1016/j.humimm.2016.02.008.
Visentin, J., Minder, L., Lee, J.-H., Taupin, J.-L., Di Primo, C., 2016d. Calibration free concentration analysis by surface plasmon resonance in a capture mode. Talanta 148, 478–485. https://doi.org/10.1016/j.talanta.2015.11.025.
Visentin, J., Couzi, L., Dromer, C., et al., 2018. Overcoming non-specific binding to measure the active concentration and kinetics of serum anti-HLA antibodies by surface plasmon resonance. Biosens. Bioelectron. 117, 191–200. https://doi.org/10.1016/j.bios.2018.06.013.
Wiebe, C., Gibson, I.W., Blydt-Hansen, T.D., et al., 2012. Evolution and clinical pathologic correlations of de novo donor-specific HLA antibody post kidney transplant. Am. J. Transpl. Off. J. Am. Soc. Transpl. Am. Soc. Transpl. Surg. 12 (5), 1157–1167. https://doi.org/10.1111/j.1600-6143.2012.04013.x.
Wu, P., Jin, J., Everly, M.J., Lin, C., Terasaki, P.I., Chen, J., 2013. Impact of alloantibody strength in crossmatch negative DSA positive kidney transplantation. Clin. Biochem. 46 (15), 1389–1393. https://doi.org/10.1016/j.clinbiochem.2013.05.053.